Spin-dependent dynamics of polaron pairs in organic semiconductors

D. R. McCamey,[*,†] S.-Y. Lee,[‡] S.-Y. Paik, J. M. Lupton, and C. Boehme
Department of Physics and Astronomy, University of Utah, 115 South 1400 East, Salt Lake City, Utah 84112, USA
(Received 29 March 2010; revised manuscript received 7 July 2010; published 13 September 2010)

We present a theoretical investigation of the effect of spin manipulation of polaron pairs (PPs) on the conductivity of organic semiconductors. Control of the PP spin state is achieved using pulsed electron-spin resonance. We demonstrate that manipulation of PPs will result in changes in the free-polaron density in the material, with corresponding changes in the conductivity due to the contribution of PP dissociation to the free-carrier density. The time-dependent form of this conductivity change following spin resonant perturbation is determined, and the effect of a number of experimental variables investigated. We find that, under certain conditions, these time-dependent current measurements reveal the dynamics of PP intersystem crossing. We compare these predictions with previous experiments on organic light-emitting diodes made of poly[2-methoxy-5-(2′-ethyl-hexyloxy)-1,4-phenylene vinylene] and conclude that PP intersystem crossing times τ_{isc} in this material may exceed 10 μs at low temperatures.

DOI: 10.1103/PhysRevB.82.125206 PACS number(s): 76.30.−v, 72.20.Jv, 72.80.Le, 73.61.Ph

I. INTRODUCTION

Semiconducting organic polymers are an interesting class of materials,[1] with a wide range of applications. Arguably, the most important of these applications is electricity-light conversion, when the material is incorporated in either an organic light-emitting diode (OLED) or an organic solar cell.[2–7] The ability of this material to perform such functions is directly related to the generation, dissociation, and recombination of polarons and polaron pairs (PPs).[8,9] Recombination of PPs is strongly influenced by the spin of the constituent polarons; in most materials those pairs in triplet spin states are unable to recombine radiatively and are thus unable to contribute to light emission in OLEDs. When the formation of pairs is dominated by spin statistics, 75% of PPs are unable to emit light and can be considered wasted. A number of ways to overcome this limitation exist, including nonstatistical pair formation[10] and intersystem crossing. However, there is still significant debate over which (if any) of these processes are important in organic semiconductors.[11–13] There is also particular uncertainty regarding the magnitude of the PP intersystem crossing time, with estimates ranging from ~100 ps (Refs. 14 and 15) to over 10 μs (Refs. 16 and 17) in poly[2-methoxy-5-(2′-ethyl-hexyloxy)-1,4-phenylene vinylene] (MEH-PPV), a typical organic semiconductor. Correctly determining the intersystem crossing rate is fundamentally important, as it is directly related to efficiency limitations in organic devices.

In this paper, we outline a simple method to quantify the intersystem crossing rate of the exciton precursor states, i.e., the rate at which PPs incoherently transitions between the singlet and triplet manifolds. We note that a similar approach has been used to determine the spin mixing rate between triplet sublevels at zero field,[18] although the relevance to organic semiconductors has not been noted. We utilize the results obtained to set an upper limit on intersystem crossing rates by inspecting data from previous studies on MEH-PPV devices.

II. SPIN MANIPULATION USING ELECTRON-SPIN RESONANCE

To investigate spins it is useful to be able to manipulate them. A technique of particular use is electron-spin resonance (ESR).[19] This technique is generally implemented by applying microwaves with a fixed frequency to a sample while an external magnetic field is swept. When the Larmor precession frequency of the spins (which is proportional to the energy splitting between spin eigenstates, as tuned by the Zeeman interaction with the magnetic field) corresponds to the frequency of the applied microwaves, the spins will precess between the eigenstates. These Rabi oscillations can occur with frequencies approaching 10^8 Hz,[20] much faster than most electronic processes involving polarons in organic materials.

While ESR is a remarkably useful tool for investigating the properties of large ensembles of spins, it has limitations when the number of spins to be investigated is small, such as in the thin films utilized for organic electronics. Due to the detection method—usually measuring the absorption of the applied microwaves—the number of spins that can be observed by standard ESR is generally considered[19,21] to be limited to $\sim 10^9$. One way to overcome the number limitation is to use ESR to manipulate the spins but to employ another method to detect the spin state. As a result, electrically detected magnetic resonance (EDMR), where the resonant excitation is applied conventionally, but detected via the effect the spin manipulation has on the device current, can allow investigation of extremely small spin ensembles in device architectures.[22] This technique has been widely used in organic semiconductors in the incoherent regime.[23–26]

Recently, we have demonstrated that it is possible to monitor the coherent manipulation of PPs between the singlet and triplet manifolds in OLEDs by measuring the effect this manipulation has on the current through the device.[27–29] A brief outline of how the spin manipulation leads to modulation of the device current was given in Ref. 27; here, we expand on this work, in particular, discussing the effect random intersystem crossing between the singlet and triplet

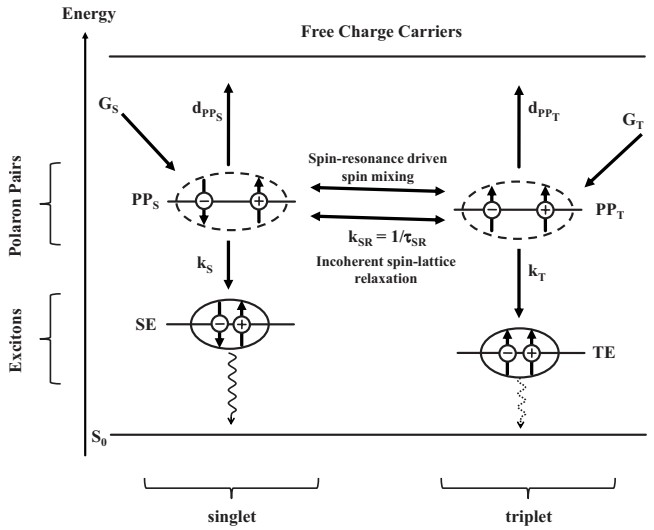

FIG. 1. Diagram showing the rates and rate coefficients of PP formation and dissociation in an organic semiconductor. Polarons travel through the material until two of them become Coulombically coupled, forming PPs of singlet (G_S) or triplet (G_T) content. These pairs may either dissociate back to free polarons (d_S, d_T) or become highly coupled, forming excitons (singlet, SE, or triplet, TE), which may recombine either radiatively or nonradiatively. PPs may undergo intersystem crossing, incoherently moving between singlet and triplet configurations due to interacting with the environment (with the rate k_{SR}).

states has on the current transients observed after coherent spin manipulation.

The results outlined here demonstrate how a simple, pulsed EDMR (pEDMR) experiment can place a lower limit on the intersystem crossing time of PPs. We then use this result to discuss recent pEDMR measurements on a number of prototypical devices based on MEH-PPV.

III. RATE EQUATIONS

In this section, we will discuss the formation, dissociation, and recombination of PPs in organic semiconductors. While we note that there is some discussion surrounding the exact nature of charge carriers in many organic materials,[30–32] in the work described here we utilize a polaron picture, as polarons are generally regarded to be the dominant charge carrier in semiconducting polymers, particularly MEH-PPV,[33] which we use here as a model system. We note that this distinction is not germane to our argument—indeed, identical arguments to those given below could be given for pairs of alternative charge carriers—such as bare electron-hole pairs—which may be present in organic semiconductors.

Figure 1 shows a diagram of the important processes. Polarons travel through the material until two of them become Coulombically coupled, forming PPs. These pairs may either dissociate back to free polarons[34] or become highly coupled, forming excitons, which may recombine either radiatively or nonradiatively. PPs may also undergo intersystem crossing, incoherently moving between singlet and triplet configurations due to interactions with the environment. Such random incoherent singlet-triplet transitions may arise, for example, due to spin-orbit coupling, although we note that spin-orbit coupling between the singlet and triplet states of Coulombically bound pairs in organic semiconductors is expected to be negligible.[35]

Figure 1 shows an idealized rate picture for a system consisting of two populations of PPs, with exclusively singlet (PP_S) or triplet (PP_T) content, and densities $n_S(t)$ and $n_T(t)$, respectively. We make no assumption regarding the time dependence of the total number of PPs, $N(t)=n_S(t)+n_T(t)$—particularly, we *do not* require that the total number of PPs is conserved.

The two sets of rate coefficients, k_S and k_T, and d_S and d_T, respectively, signify exciton and free-polaron formation, and are not assumed to be equal. We define $\Gamma_S=k_S+d_S$ and $\Gamma_T=k_T+d_T$, which we will refer to as the PP loss rate. The generation rates, G_S and G_T are assumed to be constant in time and may or may not be spin dependent (i.e., not necessarily equal). The formation of PPs may be achieved in a number of ways. Electrical injection of electron and hole polarons which form pairs due to their Coulombic interaction is assumed, in this work, to result in $G_T=3G_S$ due to the statistics of random spin selection. Alternatively, optical excitation[36] can be used to generate PPs, almost exclusively in the singlet state, in which case we would choose to set $G_T=0$ in this model.

The spin-relaxation rate, k_{SR}, characterizes the time taken for the spins to return to thermal equilibrium. This time is also often called the intersystem crossing time. As some confusion exists in the literature regarding the definition of intersystem crossing, we define it here explicitly as a "radiationless transition between two electronic states having different spin multiplicities."[37] We note that this definition does not consider the underlying physical mechanism which leads to the transition. We then define (without loss of generality) the energy difference between singlet and triplet PPs $\Delta E=E(PP_S)-E(PP_T)$. A system where the singlet has a lower energy than the triplet gives a negative ΔE. The Boltzmann factor for these populations is $f=e^{-\Delta E/k_BT}$, and we define $\rho=\frac{1}{1+f}$ as the fraction of PPs in the triplet state [which leads to $(1-\rho)$ as the fraction in the singlet state]. We note that, for spin resonance between the singlet and triplet states, $\Delta E=h\nu$, where ν is the resonant frequency.

To determine the effect of spin manipulation on this system, we model such manipulation as an instantaneous transfer of PPs from one spin state to another. By using a statistical rate picture for the resulting ensemble of spontaneous electronic transitions, we can calculate the corresponding population density dynamics as the system returns to its steady state.[38,39] This rate picture allows us to calculate the electrical conductivities σ_S and σ_T, which arise due to dissociation of singlet and triplet PPs.

IV. POPULATION DENSITY DYNAMICS

To determine the current we must first find the time-dependent PP density. To do this, we consider the standard rate equation for the PP_S and PP_T,

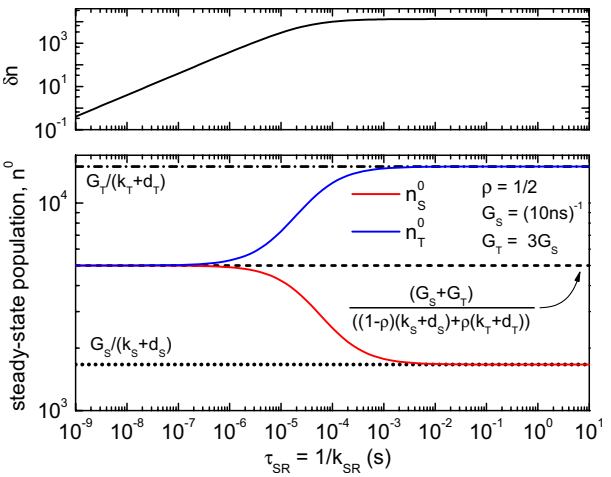

FIG. 2. (Color online) The steady-state solution for the two spin populations (bottom), and the difference in population (top) as a function of spin mixing time, for the case of electrical injection ($G_T=3G_S$). Here, $\rho=0.5$. At small τ_{SR}, the population distribution approaches the thermal distribution, and at high τ_{SR} it is determined by the generation and recombination rates.

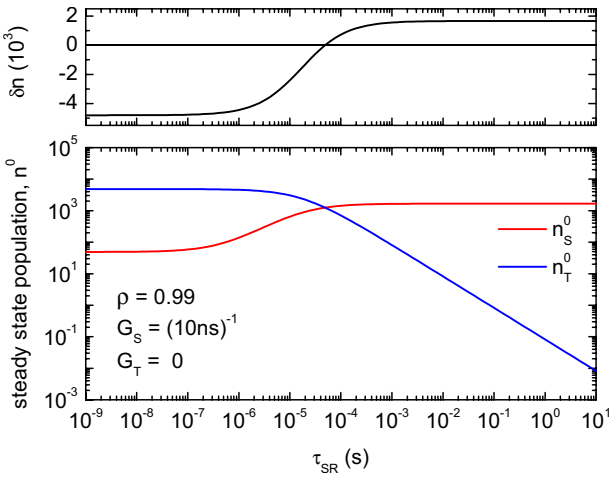

FIG. 3. (Color online) The steady-state solution for the two spin populations (bottom), and the difference in population (top) as a function of spin mixing time, for the case of optical excitation ($G_T=0$). Here, $\rho=0.99$. At small τ_{SR}, the population distribution approaches the thermal distribution, and at high τ_{SR} it is determined by the generation and recombination rates.

$$\frac{dn_S}{dt} = G_S - n_S(t)\Gamma_S - [n_S(t) - n_S^{\text{therm}}(t)]k_{SR}, \tag{1}$$

$$\frac{dn_T}{dt} = G_T - n_T(t)\Gamma_T - [n_T(t) - n_T^{\text{therm}}(t)]k_{SR}, \tag{2}$$

where $n_S^{\text{therm}}(t)=(1-\rho)N(t)$ and $n_T^{\text{therm}}(t)=\rho N(t)$, again noting that $N(t)=n_S(t)+n_T(t)$, leading to a coupled system of inhomogeneous differential equations. Note that $n_S^{\text{therm}}(t)$ and $n_T^{\text{therm}}(t)$ are used rather than the steady-state solutions, n_S^0 and n_T^0, as the total density of PPs is not constant with time.

A. Steady-state solutions

The steady-state solutions to the rate equations, found by setting $dn_S/dt=0$ and $dn_T/dt=0$, are given by

$$n_T^0 = \frac{\rho G_S k_{SR} + (\Gamma_S + \rho k_{SR})G_T}{\Gamma_S\Gamma_T + (1-\rho)k_{SR}\Gamma_S + \rho k_{SR}\Gamma_T}, \tag{3}$$

$$n_S^0 = \frac{(1-\rho)G_T k_{SR} + (\Gamma_T + (1-\rho)k_{SR})G_S}{\Gamma_S\Gamma_T + (1-\rho)k_{SR}\Gamma_S + \rho k_{SR}\Gamma_T}, \tag{4}$$

where n_S^0 and n_T^0 are the steady-state PP_S and PP_T densities, respectively.

The steady-state values are shown in Fig. 2 for $\rho=0.5$ (corresponding to $\Delta E=0$) and $G_T=3G_S$, corresponding to electrical injection of polarons, and Fig. 3 for $\rho=0.99$ (corresponding to $\Delta E\approx 4.6k_BT$) and $G_T=0$, corresponding to the case of optical excitation. Both these figures also show δn, the difference in population between PP_S and PP_T.

In the limit of very large or very small k_{SR}, we obtain the steady-state values shown in Table I. For fast k_{SR} we obtain a Boltzmann distribution between the two states (i.e., $\frac{n_S^0}{n_T^0}=\frac{1-\rho}{\rho}=f$). However, in the limit of extremely slow k_{SR} we obtain steady-state populations equivalent to two independent systems (which is indeed what we have when $k_{SR}\to 0$).

B. Solution of the rate equations

The transient solutions to the rate equations are given by

$$n_S(t) = A_1 e^{(-\Gamma_1 t)} + A_2 e^{(-\Gamma_2 t)} + n_S^0, \tag{5}$$

$$n_T(t) = B_1 e^{(-\Gamma_1 t)} + B_2 e^{(-\Gamma_2 t)} + n_T^0, \tag{6}$$

where $A_{1,2}$ and $B_{1,2}$ are amplitudes, and Γ_1 and Γ_2 are the rates defined below.

We can simplify further by noting that at $t=0$, $n_S(0)=A_1+A_2+n_S^0$ and $n_T(0)=B_1+B_2+n_T^0$. As we are interested in the transient response following resonant excitation between the PP_S and PP_T populations, we can define the change in population due to such a process as $\Delta n=[n_S(0)-n_S^0]=-[n_T(0)-n_T^0]$ since the number of PPs is conserved during the short microwave pulse which perturbs the spin populations (noting that $\Delta n\le \delta n$). This leads to $A_2=\Delta n-A_1$ and $B_2=-\Delta n-B_1$, resulting in a biexponential decay of the singlet and triplet PP densities according to

$$n_S(t) = A_1 e^{(-\Gamma_1 t)} + (\Delta n - A_1)e^{(-\Gamma_2 t)} + n_S^0, \tag{7}$$

$$n_T(t) = B_1 e^{(-\Gamma_1 t)} - (\Delta n + B_1)e^{(-\Gamma_2 t)} + n_T^0, \tag{8}$$

where the rates are given by

$$\Gamma_1 = \frac{(\Gamma_S + \Gamma_T + k_{SR}) - [(\Gamma_S - \Gamma_T)^2 + 2(2\rho - 1)k_{SR}(\Gamma_S - \Gamma_T) + k_{SR}^2]^{1/2}}{2}, \tag{9}$$

$$\Gamma_2 = \frac{(\Gamma_S + \Gamma_T + k_{SR}) + [(\Gamma_S - \Gamma_T)^2 + 2(2\rho - 1)k_{SR}(\Gamma_S - \Gamma_T) + k_{SR}^2]^{1/2}}{2}. \tag{10}$$

We note that $\Gamma_2 > \Gamma_1$.

The coefficients can be written as

$$A_1 = \frac{\Gamma_1\Gamma_T(\Gamma_S - \Gamma_2) + \Gamma_1[\rho\Gamma_T + (1-\rho)\Gamma_S]k_{SR} + \Gamma_1(1-\rho)\rho k_{SR}^2}{(\Gamma_1 - \Gamma_2)[\Gamma_S\Gamma_T + (1-\rho)\Gamma_S k_{SR} + \rho\Gamma_T k_{SR}]}\Delta n, \tag{11}$$

$$B_1 = \frac{-\Gamma_1\Gamma_S(\Gamma_T - \Gamma_2) - \Gamma_1(\Gamma_T - \Gamma_S)\rho k_{SR}}{(\Gamma_1 - \Gamma_2)[\Gamma_S\Gamma_T + (1-\rho)\Gamma_S k_{SR} + \rho\Gamma_T k_{SR}]}\Delta n. \tag{12}$$

There are a number of interesting cases to consider, particularly in the limit that k_{SR} is very large or very small. The limiting coefficients and rates are shown for these cases in Table II. The rates and coefficients obtained here will be discussed in detail in the next two sections.

V. MODELING CONDUCTIVITY USING REALISTIC EXPERIMENTAL PARAMETERS

In this section, the results obtained above will be used to model the transient form of the PP recovery to the steady state after resonance-induced perturbation of the singlet and triplet densities. For all the simulations presented here, we will use the values shown in Table III. These parameters were chosen to be similar to experimentally obtained values on MEH-PPV at low temperature,[27] recalling that $\Gamma_S = k_S + d_S$ and $\Gamma_T = k_T + d_T$. We have also chosen $\rho = 0.5$ (i.e., $|\Delta E| \ll k_B T$), corresponding to thermal energies much larger than the singlet-triplet splitting of the PPs, ΔE. The rates are considered for the case of electrical injection of charge carriers by setting $G_T = 3G_S$ to reflect the statistical generation of spin pairs from injected free polarons.

Time constants

The rate coefficients (Γ_1, Γ_2) obtained using the given parameters are plotted in Fig. 4 as a function of the intersystem crossing time, $\tau_{SR} = 1/k_{SR}$.

The limiting values of Γ_1 and Γ_2, in the limits $k_{SR} \to 0$ and $k_{SR} \to \infty$, are given in Table II. We see that, in the limit $k_{SR} \to 0$, Γ_1 and Γ_2 are equivalent to the rates that would be expected for two independent systems (which is indeed the situation we have), as illustrated in Fig. 5(a). As k_{SR} increases, a more complicated picture arises, due to the fact that as well as equilibrating as individual systems, intersystem crossing also contributes to returning the system toward the thermal distribution. A problem arises due to the fact that, while this equilibration takes place, the total number of PPs is not conserved. Thus, the transient can exist even after the thermal distribution—but not the steady-state population—is recovered. The transient in this situation is most obvious when $k_{SR} \approx (1-\rho)\Gamma_S + \rho\Gamma_T$ as this provides both a reasonable thermalization time as well as a significant change in the total PP density. The dashed lines in Fig. 4 show these limiting cases for the specific values used in that calculation.

TABLE I. Limiting values for the steady-state singlet and triplet population densities.

	$k_{SR} \to 0$	$k_{SR} \to \infty$
n_S^0	$\frac{G_S}{\Gamma_S}$	$\frac{(1-\rho)(G_S+G_T)}{(1-\rho)\Gamma_S+\rho\Gamma_T}$
n_T^0	$\frac{G_T}{\Gamma_T}$	$\frac{\rho(G_S+G_T)}{(1-\rho)\Gamma_S+\rho\Gamma_T}$

In the limit of very fast k_{SR}, the values of Γ_1 and Γ_2 approach k_{SR} and $(1-\rho)\Gamma_S + \rho\Gamma_T$, respectively. However, in this limit, it is the exponential with exponent k_{SR} which dominates; the recovery of the thermal population distribution happens so quickly that the total PP density remains effectively constant, leading to a vanishing coefficient to the longer exponential term. We will discuss this in the next section.

Finally, the analytic solution for the two rates allows us to place an upper limit on k_{SR}. We find that

$$k_{SR} < \Gamma_2 \tag{13}$$

irrespective of the value of k_{SR}, as illustrated in Fig. 4. As a result, if we are able to experimentally identify the two time constants, the spin mixing rate will be smaller than the larger of the two rates, as $\Gamma_2 > \Gamma_1$. (Alternatively, we can say that the spin mixing time will be longer than the shorter of the two biexponential lifetimes, i.e., $\tau_{SR} > 1/\Gamma_2$.)

We note that a number of the above results also hold for the case of optical generation of PPs, obtained by setting $G_T = 0$. Since the rate constants discussed in this section do not depend on the PP generation rates, the results hold for both electrical and optical generation of carriers. The impact of the type of generation is seen in the steady-state population, which determines the sign of Δn through the imbalance in the steady-state singlet and triplet PP populations. As the steady-state population is determined by the generation, dissociation, and recombination rates, k_{SR} and ΔE, dramatic changes in the generation rate will determine whether n_S^0

TABLE II. Limiting values for the rates and coefficients given in Eqs. (9)–(12).

	$k_{SR}\rightarrow 0$	$k_{SR}\rightarrow\infty$
A_1	0	$-\rho(1-\rho)\Delta n$
B_1	$-\Delta n$	0
Γ_1	Γ_T	$(1-\rho)\Gamma_S+\rho\Gamma_T$
Γ_2	Γ_S	k_{SR}

$>n_T^0$ or $n_S^0<n_T^0$. This imbalance will change the sign of the transient, but not the rate constants, provided all other rates remain the same.

VI. OBSERVATION OF POPULATION DYNAMICS BY TRANSIENT CONDUCTIVITY MEASUREMENTS

As discussed above, electrical detection of magnetic resonance requires a way to transduce the spin information of the carriers involved to the bulk conductivity. This can occur in a number of ways; spin-dependent trapping,[40] scattering,[41,42] and hopping are phenomena arising from Pauli blockade and have all been used to observe EDMR. Of particular interest in the study of organic semiconductors is spin-dependent recombination and dissociation of PPs, as these processes dominate the optoelectronic properties of these materials. These mechanisms are illustrated in Fig. 1.

We now consider the device conductivity, which is proportional to the macroscopic observable (current) in our measurement. The electrical conductivity is given by

$$\sigma = \sigma_0 + \sigma_S + \sigma_T, \tag{14}$$

where σ_0 is a large nonvarying conductivity due to all transport mechanisms present in the device, such as free polarons which are generated by electrical injection or direct optical excitation; σ_S and σ_T are the conductivities due to free carriers obtained from the dissociation of PPs for the singlet and triplet PPs, respectively. These conductivities are given by

$$\sigma_S(t) = (\mu_e + \mu_h) e \tau d_S n_S(t), \tag{15}$$

$$\sigma_T(t) = (\mu_e + \mu_h) e \tau d_T n_T(t), \tag{16}$$

where $\mu_{e(h)}$ is the mobility of a free-electron (hole) polaron, e the charge on a free carrier, n_0 the steady-state free-polaron density, and τ the free-carrier lifetime. We replace $(\mu_e+\mu_h)$ with 2μ, where $\mu=(\mu_e+\mu_h)/2$, the average carrier mobility. We note the seminal work of Bozano *et al.*[43] demonstrated that under operating conditions $\mu_e\approx\mu_h$ in MEH-PPV, although this is not a necessary assumption.

From the above equations, we can see that the conductivity due to PP dissociation is directly dependent on the density of PPs in each state. As a result, varying the PP spin populations will result in a change in the total conductivity of the device. Since we are only interested in the change in the conductivity, $\Delta\sigma$, we can ignore the steady-state component of the population and focus only on the time varying part.

The transient current following spin excitation is therefore given by

$$\Delta\sigma(t) = 2\mu e \tau [d_S n_S(t) + d_T n_T(t)] \tag{17}$$

$$= 2\mu e \tau \{ d_S [A_1 e^{-\Gamma_1 t} + (\Delta n - A_1) e^{-\Gamma_2 t}] + d_T [B_1 e^{-\Gamma_1 t} - (\Delta n + B_1) e^{-\Gamma_2 t}] \}. \tag{18}$$

The expected transient response of the current through an OLED under forward bias, as a function of the characteristic time scale for intersystem crossing, is given in Fig. 6. The parameters used for this calculation are those summarized in Table III.

It is illustrative to consider the limiting cases which are given by

$$\Delta\sigma(t) = 2\mu e \tau \Delta n [d_S e^{-\Gamma_S t} - d_T e^{-\Gamma_T t}] \tag{19}$$

for $k_{SR}\rightarrow 0$ and

$$\Delta\sigma(t) = 2\mu e \tau \Delta n [(d_S - d_T) e^{-k_{SR} t} + d_S \rho (1-\rho)(e^{-k_{SR} t} - e^{-[(1-\rho)\Gamma_S + \rho\Gamma_T]t})] \tag{20}$$

for $k_{SR}\rightarrow\infty$.

In both cases, the conductivity transient has the form of a double exponential recovery, although in the case where $k_{SR}\rightarrow\infty$, the transient signal becomes vanishingly small.

Finally, we note that, depending on the details of the light-emission process from the system, the arguments put forward above could also be made for optical detection of spin manipulation effects in organic materials[44] by replacing the dissociation rates (d_S, d_T) with the recombination rates (k_S, k_T) in Eqs. (15) and (16) and recording the photon rather than the charge flux.

VII. COMPARISON WITH EXPERIMENTAL RESULTS

We will now use these results to analyze experimentally obtained current transients in OLEDs. Figure 7 shows the resonant change in current through an MEH-PPV OLED operated in the forward bias regime (i.e., under light emission) at a temperature of 15 K. The electrical injection of charge carriers and subsequent statistical pairing of polarons results in $G_T\approx 3G_S$, the same situation as that modeled in Sec. VI above. Following spin manipulation between the singlet and triplet manifolds, the device current is observed to display the predicted enhancement-quenching transient as the singlet and triplet populations relax back to their equilibrium value,

TABLE III. Values used in the simulation of PP density and current transients, based on empirical results (Ref. 27).

Parameter	k_S	d_S	k_T	d_T	G_S
Value	$(50\ \mu s)^{-1}$	$(25\ \mu s)^{-1}$	$(150\ \mu s)^{-1}$	$(75\ \mu s)^{-1}$	$(10\ ns)^{-1}$

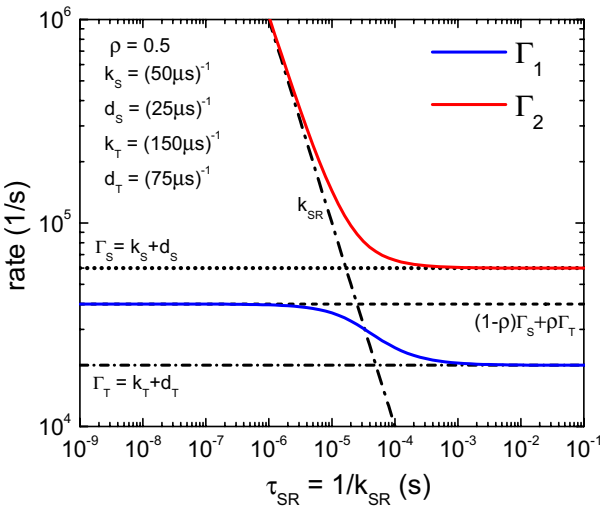

FIG. 4. (Color online) Rate coefficients, $\Gamma_{1,2}$ [see Eqs. (9) and (10)] for the double exponential transient recovery following PP population manipulation, modeled using the realistic values given in Table III. As can be seen, Γ_1 is always less than Γ_2, and Γ_2 is always greater than k_{SR}.

on time scales of $1/\Gamma_1=30.8$ μs and $1/\Gamma_2=8.5$ μs. We can be sure that the signal arises from spin pairs, due to the beating of coherent spin motion reported in Ref. 29 and that both the quenching and enhancement behaviors belong to the same process, as they have the same magnetic field dependence.[27,29] Four numerically generated transient signals are also shown for differing τ_{SR}. We find that the numerically generated transients are able to reproduce the observed transients for all $\tau_{SR}>1/\Gamma_2$. Indeed, order of magnitude variations in τ_{SR} in this region have a negligible impact on the obtained transient signals.

If, however, we attempt to include a spin mixing rate faster than $\sim$10 μs, the model is unable to reproduce the data. This is a consequence of the result shown in Eq. (13), where we see that $k_{SR}<\Gamma_2$. We can thus place a lower limit on the spin-lattice relaxation time, $\tau_{SR}>8.5$ μs. This time is much longer than what is generally assumed for such materials,[11,45] and in good agreement with recent estimates ($\tau_{SR}=30$ μs) of the spin-lattice relaxation time of MEH-PPV polarons derived from deconvoluting frequency-dependent measurements of spin-dependent *optical* processes.[12,16]

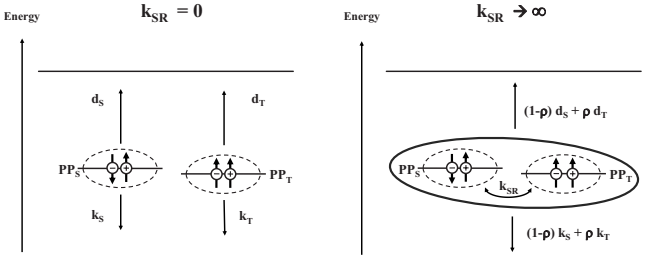

FIG. 5. The two limiting cases of spin relaxation for which the rate coefficients are determined. Intuitively, the limit for $k_{SR}\rightarrow 0$ corresponds to two independent systems, whereas the limiting case $k_{SR}\rightarrow\infty$ generates a single system with dissociation and recombination rates given by Boltzmann factor weighted averages.

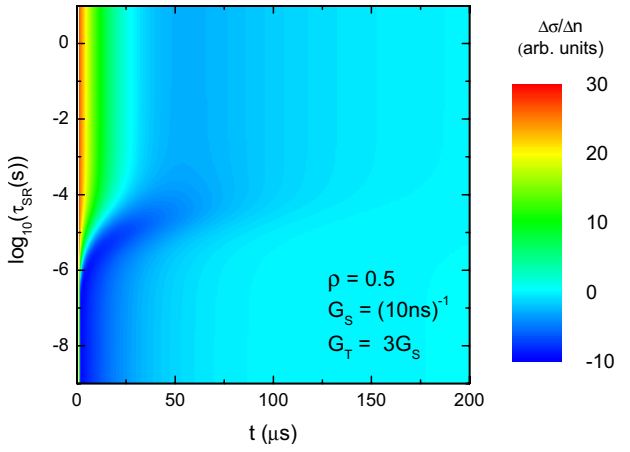

FIG. 6. (Color online) Calculated transient response of the current through a forward biased OLED following electron-spin-resonant excitation-induced mixing between the singlet and triplet PP spin configurations, as a function of time after the pulse, and the intersystem crossing time τ_{SR}. The data are modeled using the parameters noted in the figure and normalized by Δn. The transient is observed to follow an enhancement-quenching form.

Similarly, the data in Fig. 2 of Ref. 27 show the current transient following coherent excitation in an MEH-PPV OLED operated under optical illumination at zero bias. This situation corresponds to a solar cell operating in the closed

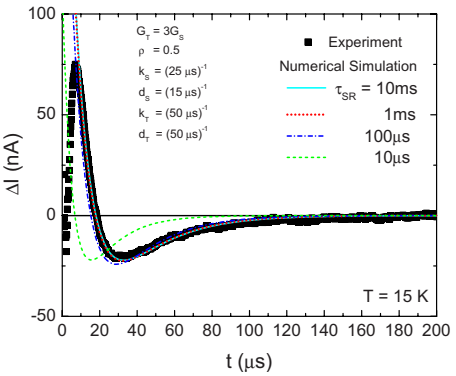

FIG. 7. (Color online) Comparison between numerically generated and experimentally measured current transients following resonant spin manipulation between the singlet and triplet states. The experimental data were obtained on an MEH-PPV OLED operating in the forward bias configuration at a temperature of 15 K. The transient has an enhancement-quenching signal, well fit by a biexponential function with time constants $1/\Gamma_1=30.8$ μs and $1/\Gamma_2=8.5$ μs. The initial rise at short times ($t<6$ μs) is due to the rise time of the amplifier used in these experiments. Numerically generated transient signal as a function of the time after microwave excitation are shown for a range of fixed intersystem crossing times τ_{SR}. The data are modeled using the parameters noted in the figure. The transient is also observed to follow an enhancement-quenching form. The magnitude of the simulated data was scaled to match the experimental data. At long τ_{SR}, variations in τ_{SR} have little effect on the form of the transient. As τ_{SR} is reduced, it begins to dominate the time constant of the enhancement part of the transient (positive ΔI). If the value of τ_{SR} used in the simulation is smaller than Γ_2, then the simulation cannot reproduce the experimental data.

circuit condition. In this configuration, we expect that $G_S \gg G_T$, resulting in a quenching-enhancement form of the current transient, opposite to that observed with electrically injected polarons. Such an inversion of the current transient is indeed observed in OLEDs acting as photodiodes,[27] when compared to OLEDs operating under electrical injection. The faster time constant of the current transient should again provide a lower limit of the spin-lattice relaxation rate. In this experiment, the fast time constant is similar to the response time of the amplifier used to measure the current, however, deconvolution of the two times gives a value of $\tau_{SR} \gtrsim 2.5$ μs. This time is in agreement with the prediction in our earlier work that $\tau_{SR} > T_2 > 0.5$ μs, where T_2 is the spin phase coherence time.[27]

VIII. CONCLUSION

We have used a statistical model to determine the expected form of the transient response of the current through an organic semiconductor device following microwave spin excitation which mixes the singlet and triplet states when electron-spin-resonance conditions are satisfied. We find that the current transient resulting from this perturbation has the form of a biexponential recovery. In particular, we find that the faster of the two time constants is always faster than the PP intersystem crossing time, and as such provides a straight forward way to place a lower limit on the spin-lattice relaxation time. We have used this result to demonstrate that, for some experimental parameters,[28] the PP intersystem crossing time exceeds 10 μs in MEH-PPV OLEDs. The investigation presented here provides a unique method for placing limits on the intersystem crossing times in PPs, as the procedure does not require the use of complicated pulse schemes, but merely the observation of transient recovery to the steady state following perturbation of the steady-state spin populations. Comparison of the result of direct measurements of the intersystem crossing rate, using electrically detected inversion-recovery pulse schemes,[46] to the observed transients would provide an important test of this model.

Finally, we note that the results presented here challenge a number of assumptions found in the literature regarding the dynamics of PPs in organic semiconductors. For example, this work is at variance with the previous assumption of equal singlet and triplet populations under optical excitation,[11,47] as such a situation would not result in a conductivity change under spin resonance.

ACKNOWLEDGMENTS

We thank William Baker for helpful discussions, as well as for providing the transient shown in Fig. 7. Acknowledgment is made to the Department of Energy (Grant No. DESC0000909) for support of this research. J.M.L. thanks the David and Lucile Packard Foundation for financial support.

*Present address: School of Physics, University of Sydney.
†dane.mccamey@sydney.edu.au
‡sylee236@physics.utah.edu

[1] V. A. Dediu, L. E. Hueso, I. Bergenti, and C. Taliani, Nature Mater. **8**, 707 (2009).
[2] C. W. Tang, Appl. Phys. Lett. **48**, 183 (1986).
[3] J. H. Burroughes, D. D. C. Bradley, A. R. Brown, R. N. Marks, K. Mackay, R. H. Friend, P. L. Burns, and A. B. Holmes, Nature (London) **347**, 539 (1990).
[4] J. Y. Kim, K. Lee, N. E. Coates, D. Moses, T.-Q. Nguyen, M. Dante, and A. J. Heeger, Science **317**, 222 (2007).
[5] D. Fyfe, Nat. Photonics **3**, 453 (2009).
[6] V. Shrotriya, Nat. Photonics **3**, 447 (2009).
[7] M. D. McGehee, Nat. Photonics **3**, 250 (2009).
[8] G. H. Gelinck, J. M. Warman, and E. G. J. Staring, J. Phys. Chem. **100**, 5485 (1996).
[9] M. Pope and C. E. Swenberg, *Electronic Processes in Organic Crystals and Polymers* (Oxford University Press, New York, 1999).
[10] S. Karabunarliev and E. R. Bittner, Phys. Rev. Lett. **90**, 057402 (2003).
[11] M. Wohlgenannt, K. Tandon, S. Mazumdar, S. Ramasesha, and Z. V. Vardeny, Nature (London) **409**, 494 (2001).
[12] M. Reufer, M. J. Walter, P. G. Lagoudakis, A. B. Hummel, J. S. Kolb, H. G. Roskos, U. Scherf, and J. M. Lupton, Nature Mater. **4**, 340 (2005).
[13] J. M. Lupton and C. Boehme, Nature Mater. **7**, 598 (2008).
[14] I. D. W. Samuel, B. Crystall, G. Rumbles, P. L. Burn, A. B. Holmes, and R. H. Friend, Chem. Phys. Lett. **213**, 472 (1993).
[15] Y. Yoshida, A. Fujii, M. Ozaki, K. Yoshino, and E. Frankevich, Mol. Cryst. Liq. Cryst. **426**, 19 (2005).
[16] C. G. Yang, E. Ehrenfreund, and Z. V. Vardeny, Phys. Rev. Lett. **99**, 157401 (2007).
[17] H.-L. Chen, Y.-F. Huang, C.-P. Hsu, T.-S. Lim, L.-C. Kuo, M. Leung, T.-C. Chao, K.-T. Wong, S.-A. Chen, and W. Fann, J. Phys. Chem. A **111**, 9424 (2007).
[18] J. Zuclich, J. U. von Schütz, and A. H. Maki, Mol. Phys. **28**, 33 (1974).
[19] C. P. Poole, *Electron Spin Resonance* (Interscience, New York, 1967).
[20] A. Schweiger and G. Jeschke, *Principles of Pulse Electron Paramagnetic Resonance* (Oxford University Press, Oxford, UK, 2001).
[21] D. C. Maier, Bruker Report **144**, 13 (1997).
[22] D. R. McCamey, H. Huebl, M. S. Brandt, W. D. Hutchison, J. C. McCallum, R. G. Clark, and A. R. Hamilton, Appl. Phys. Lett. **89**, 182115 (2006).
[23] I. Hiromitsu, Y. Kaimori, M. Kitano, and T. Ito, Phys. Rev. B **59**, 2151 (1999).
[24] G. B. Silva, L. F. Santos, R. M. Faria, and C. F. O. Graeff, *Organic and Polymeric Materials and Devices - Optical, Electrical and Optoelectronic Properties*, MRS Symposia Proceedings No. 725 (Materials Research Society, Pittsburgh, 2002), p. 4.18.

[25] G. Li, C. H. Kim, P. A. Lane, and J. Shinar, Phys. Rev. B **69**, 165311 (2004).
[26] F. A. Castro, G. B. Silva, L. F. Santos, R. M. Faria, F. Nüesch, L. Zuppiroli, and C. F. O. Graeff, J. Non-Cryst. Solids **338-340**, 622 (2004).
[27] D. R. McCamey, H. A. Seipel, S. Y. Paik, M. J. Walter, N. J. Borys, J. M. Lupton, and C. Boehme, Nature Mater. **7**, 723 (2008).
[28] C. Boehme, D. R. McCamey, K. J. van Schooten, W. J. Baker, S.-Y. Lee, S.-Y. Paik, and J. M. Lupton, Phys. Status Solidi B **11-12**, 2750 (2009).
[29] D. R. McCamey, K. J. van Schooten, W. J. Baker, S.-Y. Lee, S.-Y. Paik, J. M. Lupton, and C. Boehme, Phys. Rev. Lett. **104**, 017601 (2010).
[30] K. D. Meisel, H. Vocks, and P. A. Bobbert, Phys. Rev. B **71**, 205206 (2005).
[31] V. M. Stojanović, P. A. Bobbert, and M. A. J. Michels, Phys. Rev. B **69**, 144302 (2004).
[32] K. Hannewald, V. M. Stojanović, J. M. T. Schellekens, P. A. Bobbert, G. Kresse, and J. Hafner, Phys. Rev. B **69**, 075211 (2004).
[33] S. Kuroda, T. Noguchi, and T. Ohnishi, Phys. Rev. Lett. **72**, 286 (1994).
[34] V. I. Arkhipov and H. Bässler, Phys. Status Solidi A **210**, 1152 (2004).
[35] W. Barford, R. J. Bursill, and D. V. Makhov, Phys. Rev. B **81**, 035206 (2010).
[36] V. Dyakonov, G. Rösler, M. Schwoerer, and E. L. Frankevich, Phys. Rev. B **56**, 3852 (1997).
[37] A. D. McNaught and A. Wilkinson, *IUPAC Compendium of Chemical Terminology*, 2nd ed. (Blackwell Science, Oxford, 1997).
[38] C. Boehme and K. Lips, Appl. Phys. Lett. **79**, 4363 (2001).
[39] L. Langof, E. Ehrenfreund, E. Lifshitz, O. I. Micic, and A. J. Nozik, J. Phys. Chem. B **106**, 1606 (2002).
[40] G. W. Morley, D. R. McCamey, H. Seipel, L. C. Brunel, J. van Tol, and C. Boehme, Phys. Rev. Lett. **101**, 207602 (2008).
[41] R. N. Ghosh and R. H. Silsbee, Phys. Rev. B **46**, 12508 (1992).
[42] L. H. Willems van Beveren, H. Huebl, D. R. McCamey, T. Duty, A. J. Ferguson, R. G. Clark, and M. S. Brandt, Appl. Phys. Lett. **93**, 072102 (2008).
[43] L. Bozano, S. A. Carter, J. C. Scott, G. G. Malliaras, and P. J. Brock, Appl. Phys. Lett. **74**, 1132 (1999).
[44] L. S. Swanson, J. Shinar, A. R. Brown, D. D. C. Bradley, R. H. Friend, P. L. Burn, A. Kraft, and A. B. Holmes, Phys. Rev. B **46**, 15072 (1992).
[45] Z. Shuai, D. Beljonne, R. J. Silbey, and J. L. Bredas, Phys. Rev. Lett. **84**, 131 (2000).
[46] S.-Y. Paik, S.-Y. Lee, W. J. Baker, D. R. McCamey, and C. Boehme, Phys. Rev. B **81**, 075214 (2010).
[47] E. L. Frankevich, A. A. Lymarev, I. Sokolik, F. E. Karasz, S. Blumstengel, R. H. Baughman, and H. H. Hörhold, Phys. Rev. B **46**, 9320 (1992).